Semi-automatic Fisher-Tippett Guided Active Contour for Lumbar Multifidus Muscle Segmentation

Dorothy Lui[1], Christian Scharfenberger[1], Diana E. De Carvalho[2], Jack P. Callaghan[2], Alexander Wong[1]

***Abstract*— Rehabilitative Ultrasound Imaging or diagnostic ultrasound is used to measure geometric properties of the lumbar multifidus muscle to infer muscle strength or degeneration for back pain therapy. For this purpose, a novel semi-automatic approach (FTS: Fisher-Tippett Segmentation) based upon the Decoupled Active Contour is proposed to reliably and quickly segment the lumbar multifidus muscle in diagnostic ultrasound. To overcome speckle or hardly visible region boundaries in ultrasound images, we first propose a novel external energy functional to explicitly consider the underlying Fisher-Tippett distribution of ultrasound data. We then introduce a user-guided Hidden Markov Model trellis formation for improved segmentation of weakly-defined regions. Extensive experiments have shown that our approach not only improves the segmentation performance when compared to existing methods, but also does not rely on sub-specialized knowledge for segmentation.**

I. INTRODUCTION

Back pain is a common problem, with four out of five Canadians likely to experience back pain at least once in their lifetime [1]. One highly suspected source for back pain is posture and its impact upon back pain has been a popular research area [2], [3] Research has shown that the *lumbar multifidus muscle* is particularly important to posture and lends stability to the spine, helping to keep the body upright [4] and fine tune one's posture [5]. This thin muscle is found deep in the spine where it surrounds the torso to stabilize the joints at each level of the vertebrae. Dysfunction or weakness in this muscle group is thought to be a likely source of mechanical low back pain.

Recently, Rehabilitative Ultrasound Imaging (RUSI) or diagnostic ultrasound has been used to measure activation levels and muscle thickness [6], [7] of the lumbar multifidus muscle (see Fig. 1a). This approach is safe, non-invasive, portable and inexpensive. It allows the manual collection of quantitative measures such as muscle depth, geometry, size and symmetry to infer muscle strength or degeneration [8], [9]. For the purpose of physical therapy, this information can be useful to detect abnormalities, monitor changes in specific muscle areas during recovery [10] and to make interventional decisions. The accuracy of the information collected, however, strongly depends on the experience of the practitioner. Moreover, as image-guided therapies require little movement from the patient during acquisition, it is advantageous to have a quick approach which allows for reliable information extraction and fast segmentation of the region of interest [11]. In the case of ultrasound imaging, ultrasound inherently presents a number of challenges to region segmentation as shown in Fig. 1b including low signal-to-noise ratio (SNR), low contrast, weak boundaries, attenuation, speckle, and shadows [12]. Hence, for quantifying the muscular geometry, size, and symmetry, a user-guided segmentation approach that reduces the challenges associated with ultrasound images and ensures fast and accurate information extraction would be of great interest.

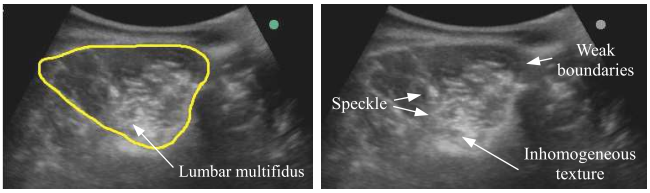

(a) (b)

Fig. 1: a) The lumbar multifidus muscle and b) challenges to segmentation such as speckle, inhomogeneous texture and weak region boundaries.

Many automatic and semi-automatic segmentation approaches have been proposed for segmenting regions of interest in ultrasound images, such as methods using texture characteristics [13], manually selected seed points located on the region boundaries and particle filtering [14], model-based initialization based on shape priors [15], and user-guided region-merging using the Fisher-Tippett distribution [16]. However, the reliance of these approaches on texture retraining to adapt them to different situations [13], strong region boundaries [14], shape priors [15], consistent textures and relatively homogeneous regions [16] makes it challenging for them to extract the lumbar multifidus muscles properly due to strong shape variabilities, speckle, inhomogeneous texture, and weak region boundaries.

Finally, interactive intelligent scissors [17] and enhanced intelligent scissors [18] have been proposed to allow the user to manually guide the contour for segmenting the image. While intelligent scissors [17] enables the contour to snap to strong neighboring structures, it can be time consuming to have the 'live wire' attract to the desired edge, especially in the presence of weak or non-existent boundaries. The enhanced intelligent scissors [18] overcomes this limitation by introducing a wavelet phase-based representation, however, assumes Gaussian-distributed data and does not consider ultrasound's Fisher-Tippett distribution [16], [19].

[1]D. Lui, C. Scharfenberger and A. Wong are with Faculty of Systems Design Engineering, Vision and Image Processing Lab, University of Waterloo, 200 University Ave. West, Waterloo, Canada dorothy.lui at uwaterloo.ca

[2]D.E. De Carvalho and J.P. Callaghan are with the Department of Kinesiology, University of Waterloo, 200 University Ave. West, Waterloo, Canada

978-1-4244-7929-0/14/$26.00 ©2014 IEEE

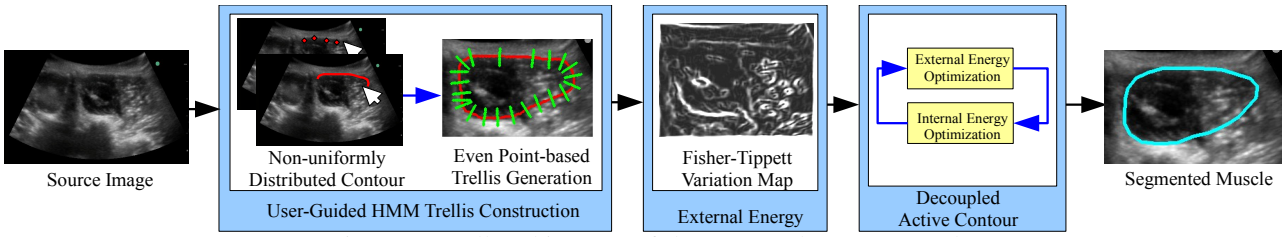

Fig. 2: Overall architecture of the proposed FTS approach

The main contribution of this work is the introduction of a novel semi-automatic approach (FTS: Fisher-Tippett Segmentation) based upon the Decoupled Active Contour (DAC) [20] to reliably and quickly segment the lumbar multifidus muscle in diagnostic ultrasound. To address the challenges associated with ultrasound images such as speckle or hardly visible region boundaries, a novel external energy functional is presented which explicitly considers the underlying Fisher-Tippett distribution of ultrasound data [16], [19] and enhances the visibility of weak region boundaries. In addition, a user-guided Hidden Markov Model (HMM) trellis formation is proposed to improve the segmentation of weakly-defined regions in ultrasound images by taking advantage of the user's guidance and expertise. The semi-automatic approach does not rely only on a sub-specialized knowledge for segmentation, but also reduces the user bias when extracting the muscle for therapy.

II. PROBLEM FORMULATION

The active contour or snake, first proposed by Kass et al [21], minimizes the energy of the snake $v(s) = (x(s), y(s)), s \in [0,1]$ where s is the normalized arc length:

$$E_{snake} = \int_0^1 \underbrace{\alpha(s)v_s^2(s) + \beta(s)v_{ss}^2(s)}_{E_{int}} - \gamma(s)E_{ext}(v(s))ds \qquad (1)$$

The internal and external energies, denoted as E_{int} and E_{ext}, respectively are composed of the first and second snake derivatives, $v_s(s)$ and $v_{ss}(s)$ and penalized by parameters $\alpha(s)$, $\beta(s)$ and $\gamma(s)$. In Mishra et al.'s [20] decoupled active contour (DAC) approach, E_{int} and E_{ext}, are optimized in separate steps to improve convergence. DAC defines a snake as a series of q discrete elements:

$$v(s_j) = v_{z_j|_{z_j=0}} = (x_{j,0}, y_{j,0}), \qquad s_j \in [0,1], j \in [1,q] \qquad (2)$$

where z_j is the corresponding j^{th} state of the j^{th} snake element. These states enable external energy optimization through formulation as a Hidden Markov Model (HMM) that is solved using dynamic programming. A trellis construction is defined where at each discrete snake element, a trellis or set of $u+1$ points lying normal to the snake are constructed as shown in Fig. 2. The series of trellises form a set of $(u+1)^q$ possible snakes where each snake passes through a given sequence of states and are penalized using state transition probabilities. A prior is then enforced through internal energy optimization using linear Bayesian estimation. However, DAC is an automatic active contour approach which is not suited for the challenging nature of segmenting lumbar multifidus muscle ultrasound data (as shown in Fig. 1b). Hence, a user-guided approach that accounts for the inherent characteristics of ultrasound images is desired.

III. METHODOLOGY

The proposed semi-automatic segmentation approach, Fisher-Tippett Segmentation (FTS) explicitly takes advantage of user guidance and ultrasound's Fisher-Tippett distribution to improve and speed up the segmentation of lumbar multifidus muscles in ultrasound. The overall architecture is shown in Figure 2 and can be divided into the following three steps: 1) *User-guided HMM trellis construction*, 2) *Computation of the external energy functional*, and 3) *Contour estimation using DAC*.

A. User-guided HMM trellis construction

A set of user guided points, $C = \{s_0, s_1, \cdots, s_n\}$ are used to derive a snake as proposed in DAC, composed of q uniformly-distributed discrete elements, $\hat{C}(s)$. The initial randomly dispersed user guided points, C, requires further derivation for two reasons. Uniformly distributed elements:

1) Allow for a sufficient number of points to aptly characterize the boundary of interest
2) Control the density of points, as too many points can be computationally expensive

In the implementation of the proposed algorithm, a periodic interpolating cubic spline [22] was used to derive the uniformly distributed snake. Then, trellises can be constructed for each discrete element of the user-guided snake to prepare the HMM for external energy optimization.

B. Computation of the external energy functional

Following the user-guided trellis construction, the HMM transition probabilities can be determined using the external energy functional and the proximity to the user-guided snake. In the proposed approach, the external energy functional employs the underlying Fisher-Tippett distribution of the ultrasound data to highlight structure based on its likelihood. The Fisher-Tippett likelihood can be described as:

$$p(x|\mu,\beta) = \frac{1}{\beta}\exp\Big(-\big(z+\exp(-z)\big)\Big), \text{where } z = \frac{x-\mu}{\beta} \qquad (3)$$

where x is an image pixel and μ and β denote the mean and positive scaling factors respectively. Since we are interested in distinctive structure to guide the external energy optimization, we define the external energy (shown in Fig. 2) as the likelihood that x is not a realization of μ and β:

$$E_{ext} = 1 - p(x|\mu,\beta) \tag{4}$$

Extensive empirical testing shows that $\beta = 0.5$ provides strong segmentation results. Each snake element's state, z_j, is then associated with a state transition probability $z_j \rightarrow z_{j+1}$ as proposed in [23] however with consideration of the proximity to the user-guided snake:

$$p(z_j, z_{j+1}) = \begin{cases} 1 & \text{if } z_j \in [-\frac{u_g}{2}, \frac{u_g}{2}] \\ 0 & \text{otherwise} \end{cases} \tag{5}$$

where u_g is a set range in proximity to the user-guided snake. The snake is then prepared for final contour estimation.

C. Contour estimation using DAC

Once the user-guided HMM trellis construction and external energy functional are defined, the DAC approach is applied for contour estimation. In the DAC approach, dynamic programming is used to optimize the HMM. This is followed by internal energy optimization which enforces a prior to the snake using linear Bayesian estimation.

IV. EXPERIMENTAL RESULTS

To evaluate the proposed approach, ten users (a mix of novices and experts) were asked to segment one of the lumbar multifidus muscles in 10 ultrasound images. Ultrasound images were collected from ten patients in maximum flexed and pelvic seat positions using a 5 MHz curvilinear array probe in B-mode. The muscles were imaged at the level of L4/L5 bilaterally in the transverse plane with the transducer oriented vertically and lateral to the spinous process. The transducer then angled slightly towards the junction between the transverse and spinous processes until the lumbar mutlifidus muscles were identified. This study was approved by the University of Waterloo ethics board. For each patient case, two segmentation attempts were executed for consistent segmentations using the semi-automatic segmentation approaches listed below:

FTS$_{FH}$ (Freehand): The proposed approach FTS is initialized using a freehand drawing contour tool where the user drags the cursor across the image to create a contour.

FTS$_{Cl}$ (Click): A second variation to FTS$_{FH}$ required the user to initialize the contour using a series of point clicks.

Enhanced intelligent scissors (EIS) [18]: The user selected points initialized in FTS$_{Cl}$ were used to initialize EIS.

Intelligent scissors (IS) [17]: A third-party implementation of IS was used for testing [24].

The ground truth segmentations used for this study were provided by a chiropractic radiologist with 9 years of professional work experience and then shown to the users prior to segmentation and hidden during segmentation. This enabled novice users to better visualize the general vicinity of the muscle location. The number of selected points and the total segmentation time for each approach were recorded. The precision, recall and F1-measure (as applied in [23]) were then calculated based on the final segmentations. Tests were completed using MATLAB on an Intel(R) Core(TM) i7 – 4770 CPU@3.40 GHz computer with 16.0 GB of RAM. The average results for each tester are shown in Table I and Fig. 3.

EIS had the highest average precision across all iterations, however had the lowest average recall and F1-measures indicating that EIS tended to undersegment regions of interest. In contrast, IS had the greatest F1-measure and recall results yet required more patience from the user to complete the segmentations, taking at least two times longer than the other approaches. The freehand FTS$_{FH}$ approach demonstrated the fastest segmentation time and was found by users to allow more control in guiding the contour and offered a better contour visualization compared to the point clicking FTS$_{Cl}$.

Besides the speed and visualization provided by FTS$_{FH}$, the users found clicking to be beneficial for precisely placing points in regions where the contour should be without having to carefully outline the entire contour. One user found that the increased speed of the freehand approach required more knowledge in placing the initial contour, while continuous feedback during segmentation provided by IS helped to better place the initial contour. In addition, it was found that the IS approach worked well in the presence of strong edges, however in the absence of strong boundaries, the user needed to include a greater number of anchoring points (as shown in Fig. 4). This resulted in jagged segmentations that do not aptly represent the contour of a muscle. In contrast, EIS and FTS derived more smooth boundaries with FTS$_{Cl}$ exhibiting the second highest F1-measure. The results of our evaluation show that FTS combines speed with high F1-measure, recall, and precision results while offering two viable alternatives to initializing the contour catering to personal preferences.

V. CONCLUSIONS

A fast and accurate semi-automatic approach called Fisher-Tippett Segmentation (FTS) is presented for segmenting the lumbar multifidus muscle. FTS extends upon the decoupled active contour [20] and utilizes user-selected points to initialize a Hidden Markov Model for extracting region boundaries. FTS also introduces a novel external energy functional that considers ultrasound's underlying Fisher-Tippett distribution to determine structurally unique regions.

Through extensive user comparisons with enhanced intelligent scissors (EIS) and intelligent scissors (IS), it was found that both the freehand and point clicking variations of FTS demonstrated fast segmentation with comparable performance against existing approaches. Although some users found IS's continuous feedback useful during segmentation, IS was the slowest method requiring patience and care especially in regions with weak boundaries. In contrast, FTS was fast to initialize and provided an accurate segmentation.

ACKNOWLEDGMENT

This research was funded by the Canada Research Chairs program, the Natural Sciences and Engineering Research Council (NSERC) of Canada and the Ontario Ministry of Research and Innovation. We would also like to thank our

TABLE I: Performance evaluation of the compared semi-automatic segmentation approaches. The highest scores are marked in bold.

User	F1-measure				User Points[a]			Total Segmentation Time [s]			
	FTS_{FH}	FTS_{Cl}	EIS	IS	FTS_{Cl}	EIS	IS	FTS_{FH}	FTS_{Cl}	EIS	IS
1	0.911	**0.919**	0.893	0.914	8	8	7	**7.95**	9.60	9.47	23.10
2	0.857	0.858	0.849	**0.870**	11	11	10	**8.03**	8.98	8.84	22.34
3	0.911	0.929	0.926	**0.931**	14	14	14	**9.94**	13.89	13.74	34.50
4	0.911	**0.914**	0.911	0.912	16	16	16	**11.87**	16.73	16.58	41.09
5	0.896	**0.925**	0.912	0.904	11	11	10	**7.36**	9.34	9.21	29.42
6	0.902	**0.919**	0.919	0.916	18	18	9	**10.60**	16.59	16.42	27.37
7	0.904	0.900	0.900	**0.916**	14	14	17	**12.64**	21.29	21.14	45.18
8	0.856	0.830	0.825	**0.884**	30	30	10	**13.50**	23.63	23.41	42.81
9	0.919	**0.926**	0.920	0.925	26	26	12	**15.47**	23.23	23.03	37.47
10	0.899	0.917	0.910	**0.922**	16	16	14	**9.86**	12.01	11.86	38.30
Avr	0.897	0.904	0.896	**0.909**	16	16	12	**10.72**	15.53	15.37	34.16

[a] FTS_{FH} was not included as it does not require individual point selection.

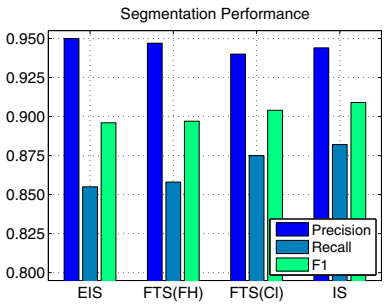

Fig. 3: Precision, recall and F1-measure evaluation of the compared approaches.

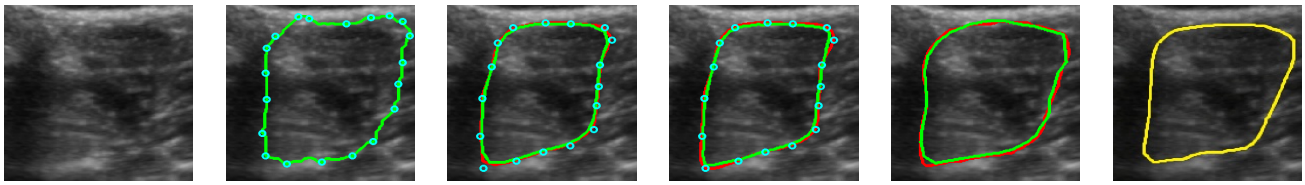

Fig. 4: Initial (red), final (green) and groundtruth (yellow) contours with clicked points (cyan) are shown. FTS_{Cl} and IS demonstrated the highest F1-measure scores however IS required many anchor points when segmenting weak boundaries.

segmentation testers for helping us complete the user guided segmentations.

REFERENCES

[1] Statistics Canada, "Back pain," Apr 2006.

[2] P. B. OSullivan, T. Mitchell, P. Bulich, R. Waller, and J. Holte, "The relationship beween posture and back muscle endurance in industrial workers with flexion-related low back pain," *Manual therapy*, vol. 11, no. 4, pp. 264–271, 2006.

[3] P. J. Mork and R. H. Westgaard, "Back posture and low back muscle activity in female computer workers: a field study," *Clinical biomechanics*, vol. 24, no. 2, pp. 169–175, 2009.

[4] S. R. Ward, C. W. Kim, C. M. Eng, L. J. GottschalkIV, A. Tomiya, S. R. Garfin, and R. L. Lieber, "Architectural analysis and intraoperative measurements demonstrate the unique design of the multifidus muscle for lumbar spine stability," *The Journal of Bone & Joint Surgery*, vol. 91, no. 1, pp. 176–185, 2009.

[5] N. Bogduk, *Clinical anatomy of the lumbar spine and sacrum*. Elsevier Health Sciences, 2005.

[6] K. B. Kiesel, T. L. Uhl, F. B. Underwood, D. W. Rodd, and A. J. Nitz, "Measurement of lumbar multifidus muscle contraction with rehabilitative ultrasound imaging," *Manual therapy*, vol. 12, no. 2, pp. 161–166, 2007.

[7] J. L. Whittaker, D. S. Teyhen, J. M. Elliott, K. Cook, H. M. Langevin, H. H. Dahl, and M. Stokes, "Rehabilitative ultrasound imaging: understanding the technology and its applications," *journal of orthopaedic & sports physical therapy*, vol. 37, no. 8, pp. 434–449, 2007.

[8] J. Hides, C. Gilmore, W. Stanton, and E. Bohlscheid, "Multifidus size and symmetry among chronic lbp and healthy asymptomatic subjects," *Manual therapy*, vol. 13, no. 1, pp. 43–49, 2008.

[9] D. S. Teyhen, J. D. Childs, M. J. Stokes, A. C. Wright, J. L. Dugan, and S. Z. George, "Abdominal and lumbar multifidus muscle size and symmetry at rest and during contracted states normative reference ranges," *Journal of Ultrasound in Medicine*, vol. 31, no. 7, pp. 1099–1110, 2012.

[10] M. Stokes, G. Rankin, and D. Newham, "Ultrasound imaging of lumbar multifidus muscle: normal reference ranges for measurements and practical guidance on the technique," *Manual therapy*, vol. 10, no. 2, pp. 116–126, 2005.

[11] N. Ben-Zadok, T. Riklin-Raviv, and N. Kiryati, "Interactive level set segmentation for image-guided therapy," in *Biomedical Imaging: From Nano to Macro, 2009. ISBI'09. IEEE International Symposium on*. IEEE, 2009, pp. 1079–1082.

[12] J. A. Noble and D. Boukerroui, "Ultrasound image segmentation: a survey," *Medical Imaging, IEEE Transactions on*, vol. 25, no. 8, pp. 987–1010, 2006.

[13] J. Olivier and L. Paulhac, *3D Ultrasound Image Segmentation: Interactive Texture-Based Approaches*, ser. Medical Imaging, D. O. F. Erondu, Ed. InTech, 2011.

[14] D. Angelova and L. Mihaylova, "Contour segmentation in 2d ultrasound medical images with particle filtering," *Machine Vision and Applications*, vol. 22, no. 3, pp. 551–561, 2011.

[15] H. M. Ladak, F. Mao, Y. Wang, D. B. Downey, D. A. Steinman, and A. Fenster, "Prostate boundary segmentation from 2d ultrasound images," *Medical physics*, vol. 27, no. 8, pp. 1777–1788, 2000.

[16] A. Wong and J. Scharcanski, "Fisher–tippett region-merging approach to transrectal ultrasound prostate lesion segmentation," *Information Technology in Biomedicine, IEEE Transactions on*, vol. 15, no. 6, pp. 900–907, 2011.

[17] E. N. Mortensen and W. A. Barrett, "Interactive segmentation with intelligent scissors," *Graphical models and image processing*, vol. 60, no. 5, pp. 349–384, 1998.

[18] A. Mishra, A. Wong, W. Zhang, D. A. Clausi, and P. Fieguth, "Improved interactive medical image segmentation using enhanced intelligent scissors (eis)," in *Proceedings of the IEEE Conference on Engineering in Medicine and Biology Society*, Aug 2008, pp. 3083 – 3086.

[19] O. V. Michailovich and D. Adam, "A novel approach to the 2-d blind deconvolution problem in medical ultrasound," *Medical Imaging, IEEE Transactions on*, vol. 24, no. 1, pp. 86–104, 2005.

[20] A. K. Mishra, P. W. Fieguth, and D. A. Clausi, "Decoupled active contour (dac) for boundary detection," *Pattern Analysis and Machine Intelligence, IEEE Transactions on*, vol. 33, no. 2, pp. 310–324, 2011.

[21] M. Kass, A. Witkin, and D. Terzopoulos, "Snakes: Active contour models," *International journal of computer vision*, vol. 1, no. 4, pp. 321–331, 1988.

[22] E. T. Lee, "Choosing nodes in parametric curve interpolation," *Computer-Aided Design*, vol. 21, no. 6, pp. 363–370, 1989.

[23] D. Lui, C. Scharfenberger, K. Fergani, A. Wong, and D. Clausi, "Enhanced decoupled active contour using structural and textural variation energy functionals," *Image Processing, IEEE Transactions on*, vol. 23, no. 2, pp. 855–869, Feb 2014.

[24] C. Wueslin, "Livewire (intelligent scissors) roi creation," MATLAB File Exchange, Apr 2013. [Online]. Available: http://www.mathworks.com/matlabcentral/fileexchange/41084-livewire-intelligent-scissors-roi-creation